nature physics

INSIGHT | REVIEW ARTICLES

PUBLISHED ONLINE: 2 APRIL 2012 | DOI: 10.1038/NPHYS2259

Quantum simulations with ultracold quantum gases

Immanuel Bloch[1,2]*, Jean Dalibard[3] and Sylvain Nascimbène[1,3]

Ultracold quantum gases offer a unique setting for quantum simulation of interacting many-body systems. The high degree of controllability, the novel detection possibilities and the extreme physical parameter regimes that can be reached in these 'artificial solids' provide an exciting complementary set-up compared with natural condensed-matter systems, much in the spirit of Feynman's vision of a quantum simulator. Here we review recent advances in technology and discuss progress in a number of areas where experimental results have already been obtained.

Calculate or simulate? Predicting the evolution of a multi-component system is often a challenge that can be solved either by direct mathematical analysis or by a device that simulates its behaviour. In many cases the latter approach may offer a faster solution, better accuracy and/or a more illustrative representation than possible with available numerical methods. A celebrated example is the ensemble of astronomical clocks that were built in Asia and Europe in the period between 1000 and 1500. They were used to predict the position of the planets and the constellations, the phases of the moon and its eclipses.

The general interest in the simulation of physical phenomena has been greatly revitalized during the past decade. This renaissance results from the conjunction of new needs and new tools. The new needs originate in the increasing role of quantum effects in the states of matter relevant for modern technology[1]. The computational power required to describe an assembly of particles in quantum physics increases exponentially with the number of its constituents. The numerical description of a sample of quantum matter is thus often limited to a small number of constituents, and this may prevent one from addressing with the desired accuracy important phenomena such as high-T_c superconductivity.

The new tools have emerged thanks to recent advances in the control of atomic gases. Here, we will restrict ourselves to the case of neutral atom assemblies, well suited for the analog simulation of complex quantum systems. The design of an analog simulator starts with the proper mapping of the Hamiltonian of the system to be simulated. This includes both single-particle physics and the interaction between the constituents. Next, one should prepare the simulator in a state which is relevant for the physical problem of interest. This can be a well-identified quantum state (for example, the ground state) or an equilibrium state at non-zero temperature. Finally, one must perform measurements on the simulator with the highest-possible precision. We show that quantum atomic gases provide a unique way to fulfil all the stages of this programme.

We have chosen three topics to illustrate the power of cold-atom assemblies for implementing analog quantum simulation. The first one deals with the control of interactions provided by Feshbach resonances. We focus on the very strongly interacting regime, where the fluid becomes scale-invariant and its behaviour is characterized by a few dimensionless coefficients. This gas forms a simulator for other strongly interacting fluids, a notion that is validated by comparing the measured coefficients with the results of state-of-the-art quantum Monte Carlo calculations. The second topic deals with the control of the energy landscape at the level of the single-particle Hamiltonian. We choose the paradigmatic example of optical lattices to explore quantum phase transitions, such as the passage from a superfluid to a Mott insulator. Single-atom control and detection allow one to study the time evolution of these strongly correlated fluids, a very difficult task for a program running on a classical computer. The last topic is the control of the topology in which the quantum fluid evolves. Artificial gauge fields can be applied to the gas, opening the way to the simulation of quantum Hall systems and of topological insulators, their time-reversal-invariant generalization. Artificial fields can reach values well above those achievable for electrons moving in a real crystal, thus illustrating another important feature of a simulator: it enables the exploration of parameter ranges well beyond what is achievable with the initial system.

Ultracold Fermi gases

We first consider quantum simulation of ultracold Fermi gases with attractive interactions. These gases constitute a model system of interacting fermions, whose physical behaviour is very rich[2–4]. The phenomenon of Feshbach resonance provides a means to tune the strength of interactions between atoms over several orders of magnitude by means of an external magnetic field. This leads to the possibility of investigating different regimes of superfluidity with a single physical system. In the case of ultracold gases, interatomic interactions can be described using a single parameter, the so-called scattering length a. The other natural length scale to consider in a Fermi gas is its inverse Fermi momentum k_F^{-1}, which is essentially equal to the mean interparticle distance. The physical behaviour of a Fermi gas is then governed by the ratio $1/(k_F a)$ of these two lengths.

In the case of weakly attractive interactions ($1/k_F a \to -\infty$), the superfluid behaviour of the gas can be understood using the Bardeen–Cooper–Schrieffer (BCS) theory of pairing[5]. Developed in the 1950s, this theory has proven extremely successful for the understanding of conventional superconductors, and constitutes a starting point for modelling more complex systems. BCS superfluidity originates from the weak pairing of particles into Cooper pairs, which are made of two particles of opposite spin and velocity (Fig. 1a).

In the other limit of interaction strength ($1/k_F a \to +\infty$), atom pairs are so strongly bound that one can picture the gas as an ensemble of molecules of which the internal structure does not play a crucial role. As these molecules are made of two fermions, they behave as bosonic particles and form a Bose–Einstein condensate (BEC) at low temperature. It is important to mention that although the attraction between atoms is very strong, the molecules themselves are weakly interacting.

[1]Fakultät für Physik, Ludwig-Maximilians-Universität, Schellingstrasse 4, 80799 München, Germany, [2]Max-Planck-Institut für Quantenoptik, Hans-Kopfermann-Strasse 1, 85748 Garching, Germany, [3]Laboratoire Kastler Brossel, CNRS, UPMC, Ecole Normale Supérieure, 24 rue Lhomond, 75005 Paris, France. *e-mail: immanuel.bloch@mpq.mpg.de.

NATURE PHYSICS DOI:10.1038/NPHYS2259

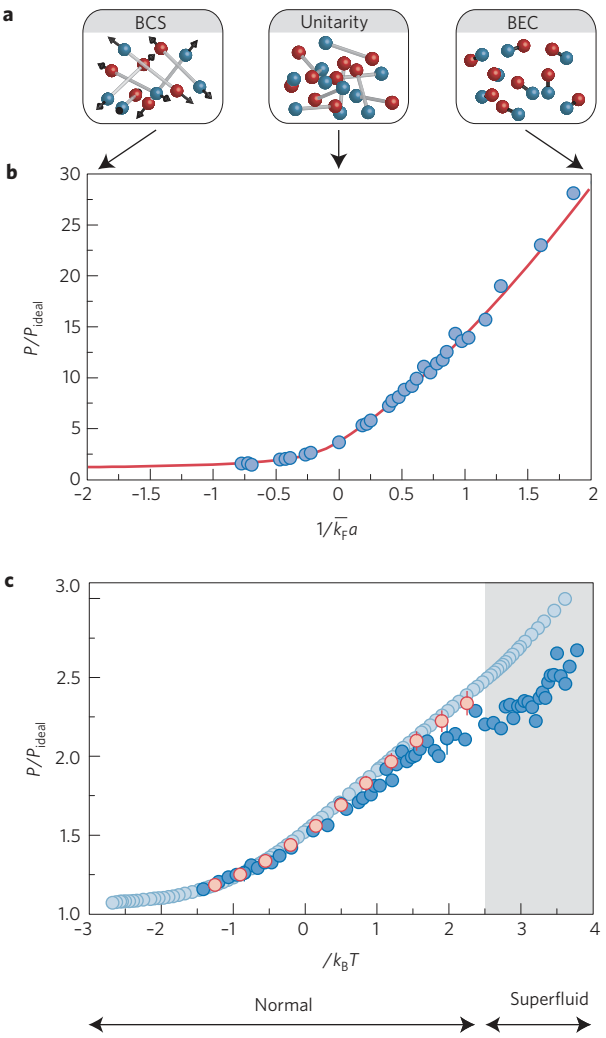

Figure 1 | Equations of state of interacting ultracold Fermi gases. **a**, Schematic representation of the BEC–BCS crossover. For weak attractive interactions, atoms of opposite spin and momentum form Cooper pairs whose spatial extent greatly exceeds the mean interparticle distance. In the opposite limit of strongly attractive interactions, the gas is made of tightly bound molecules forming a BEC. In the middle of the crossover between the BCS and BEC regimes, the scattering length diverges at the unitary limit, leading to a strongly correlated state of matter. **b**, Equation of state of the ground state of a Fermi gas in the BEC–BCS crossover, expressed as the pressure normalized by the non-interacting pressure as a function of the interaction parameter $1/\overline{k_F}a$. (For the definition of the Fermi momentum $\overline{k_F}$, see ref. 18.) The solid red line is obtained from the fixed-node diffusion Monte Carlo simulation of ref. 140 and the blue dots are experimental data from ref. 18. Panel reproduced with permission from ref. 18, © 2010 AAAS. **c**, Finite-temperature equation of state of the unitary Fermi gas. The dark (light) blue dots are the experimental data from ref. 40 (ref. 19) and the red dots are the bold diagrammatic Monte Carlo data from ref. 41. The grey area indicates the superfluid phase; the location of the normal/superfluid phase transition is taken from ref. 19. Panel reproduced with permission from ref. 19, © 2012 AAAS.

The regime of large scattering lengths ($1/k_F|a| \lesssim 1$) interpolates between these two well-understood behaviours and constitutes the so-called BEC–BCS crossover. In this regime the gas is strongly interacting and its theoretical understanding defies standard many-body techniques. Analytical results for these systems are relatively rare, limited either to a few particles[6,7] or to short-range correlations for the many-body problem[8]. As the interaction energy is comparable to the Fermi energy, there is no small parameter in the system and standard many-body techniques based on perturbation expansions cannot be used.

As a first example of a quantum simulation, let us first focus on the specific case of a Fermi gas with resonant interactions ($a = \infty$), the so-called 'unitary limit'. The scattering length being infinite, it does not appear in the equation of state of the gas; hence at low temperature one is left with just two energy scales, the chemical potential μ and the Fermi energy E_F. These quantities are then necessarily proportional, resulting in a simple expression for the equation of state $\mu = \xi E_F$. The quantity ξ is a dimensionless number that describes the full thermodynamic properties of a unitary Fermi gas[9]. It is expected to be independent of the elementary constituents of the gas, as long as they interact with short-range interactions described by an infinite scattering length. This universal character of ξ makes it relevant not only in the cold-atom context but also for modelling low-density neutron matter in the crust of neutron stars, despite densities twenty-five orders of magnitude larger than cold-atom systems[10]. The measurement of the parameter ξ constitutes a simple prototype of a quantum simulation with ultracold atoms.

Taking advantage of the simple form of the universal equation of state, the parameter ξ was extracted experimentally from various observables, such as the dynamics of the gas after release from the trap[11–13], the *in situ* cloud size[14,15], the speed of sound[16], or direct measurement of the equation of state[17–19]. These measurements agree within 5% on the value $\xi \simeq 0.4$. The good precision achieved in experiments allows one to discriminate between the various existing theoretical predictions for the parameter ξ. Whereas simple mean-field theories provide a poor quantitative description of the unitary gas because of the strong interactions, variational Monte Carlo methods are in very good agreement with the experimental results (Fig. 1; refs 20,21).

The quantum simulation of low-temperature Fermi fluids was also extended to arbitrary values of the scattering length a. The ground-state equation of state was measured in the whole BEC–BCS crossover through a study of collective mode frequencies[22,23] and a measurement of the gas pressure[18]. Once again these data were found in good agreement with Monte Carlo simulations. The quantum simulation was also extended to other observables, such as the spin susceptibility[24,25], and to the case of Fermi gases with imbalanced spin populations[15,18,26–30].

The theoretical understanding of finite-temperature effects is even more difficult and until recently no consensus was established for the equation of state[31–37]. Measurements of the equation of state in the unitary limit[13,19,38–41] thus proved useful in discriminating between various theoretical approaches. Remarkably, the precision of several per cent achieved in recent measurements[40,41] led to the validation of the diagrammatic Monte Carlo technique[41] (Box 1 and Fig. 1c). Moreover, the high-temperature virial expansion of the equation of state extracted from these experimental data could also be compared with to theoretical studies of strongly interacting few-body systems[42–44]. Similarly to the case of liquid ^{4}He, a lambda-shaped feature was observed in the equation of state at the superfluid transition[19], the theoretical understanding of which requires improvements in the precision of numerical simulations.

Detailed comparison between experiment and theory remains to be performed in the whole parameter space of interaction strength, temperature and spin imbalance. Moreover, new kinds of Fermi systems are currently being developed, such as two-component Fermi gases with mass-imbalanced effective spins and three-component Fermi gases. The first precision measurements on these systems were recently performed in ref. 45 with spin-imbalanced ^{40}K–^{6}Li mixtures. Qualitatively new physical

Box 1 | Measuring the equation of state.

One of the defining characteristics of a quantum simulator is the ability to perform high-precision measurements of key observables. The combined measurement of several intensive quantities, such as the gas density n, chemical potential μ and temperature T, allows one to reconstruct the equation of state $n(\mu, T)$ of the investigated system.

New techniques have recently been developed to extract with good precision the equation of state of an ultracold gas from its *in situ* density profile. In most cases, the atomic gas is held in a harmonic trap V generated from a magnetic field curvature or a focused laser beam. Hence, the gas density profile is non-uniform, and the atom distribution is determined by the conditions of local hydrostatic equilibrium

$$\mathrm{d}P = -n\,\mathrm{d}V, \qquad \mathrm{d}T = 0$$

The Gibbs–Duhem relation $\mathrm{d}P = S\,\mathrm{d}T + n\,\mathrm{d}\mu$ leads to the relation $\mathrm{d}\mu = -\mathrm{d}V$; that is, the local chemical potential varies as the trapping potential. A position-resolved measurement of thermodynamic quantities thus provides, from a single image, the equation of state for all chemical potential values.

It is not obvious how to measure the thermodynamic quantities n, P, and T from the recorded density profile. Indeed, standard atom imaging provides a two-dimensional profile of the density integrated along the line of sight of the probe beam. Reconstructing the atom density n requires one to invert the integration process using an Abel transformation[19,28,41]. Alternatively, the pressure P can be directly obtained by once again integrating the atom density along one direction of the two-dimensional profile[18,19,40,141,142] (Fig. B1). Finally, the temperature can be extracted, either by using an auxiliary ultracold gas whose equation of state is known well and which is at thermal equilibrium with the gas of interest[40,143], or from the low-density regions of the trapped gas where interaction effects are weak[19,41].

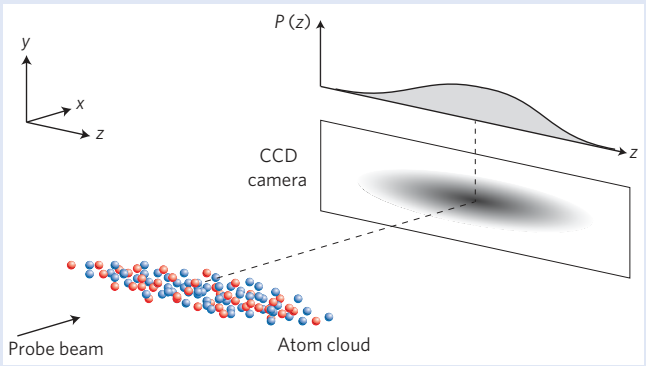

Figure B1 | Measuring the local pressure inside a trapped gas. The CCD (charge-coupled device) camera signal corresponds to the atom density integrated along the line of sight x. An further integration along y provides a one-dimensional profile, which is proportional to the local gas pressure $P(z)$ inside the gas along the z axis.

behaviours are expected to occur with these systems, making this branch of quantum simulation an exciting direction of research over the coming years.

Optical lattices

In a typical condensed-matter system, electrons can be modelled as moving on a lattice generated by the periodic array of atom cores. Such a general setting can be simulated with ultracold atoms using the concept of an 'optical lattice'[46]. Here, the periodic potential through which the particles move is generated externally by making use of the interference pattern of overlapping laser beams. The alternating bright and dark regions of such an interference pattern are experienced by the atoms as a periodic potential through the optical dipole force. For large-enough detunings from an atomic transition frequency, such optical light fields can be considered to be purely conservative and defect-free potentials. By superimposing laser fields at various angles, any lattice geometry that can be conceived by Fourier synthesis can thereby be realized in the experiments[47]. So far, experiments have mainly focused on simple cubic-type lattices, which can be generated by superimposing three independent standing waves[48]. However, recently, also superlattice structures[49,50], triangular[51], hexagonal[51,52] and Kagomé[53] lattices have been realized. The band-structure and topology of these lattices can be tuned *in situ*, for example, by simply changing the intensity, frequency or phase of the superimposed laser fields. One of the latest examples of this type of tunability includes the controlled movement and merging of Dirac cones on a hexagonal lattice[52]. This unique degree of optical control of the lattice structure also allows one to time-modulate the lattice potentials in space. The resulting time-averaged effective tunnel couplings can be tuned by the modulation strength and frequency[54,55] and have enabled the experimental control of the magnitude and sign of the tunnel coupling between lattice sites[56,57].

Things become even more interesting when interactions come into play. As neutral atoms typically only experience short-ranged collisional interactions, these can be efficiently described as on-site interactions. Only when two or more particles meet on a lattice site do they take note of the interaction induced by the collisional partner. The Hamiltonian of such interacting ultracold atoms on a lattice is given by the Hubbard model, which serves as one of the most prominent models for a solid in condensed-matter physics[46,58–61]. In this model, the hopping between neighbouring sites is characterized by a tunnel coupling J and an on-site interaction energy U. For the case of bosons and repulsive interactions ($U > 0$) the system undergoes a quantum phase transition from a superfluid to a Mott insulator as the ratio of interaction to kinetic energy U/J is tuned above a critical interaction strength[62–64]. This can be best understood by noting that, in the strongly interacting regime, density fluctuations become energetically costly and are therefore suppressed. In the extreme, so-called 'atomic limit', where the kinetic energy vanishes, the ground state of the system corresponds to a lattice gas with integer filling per lattice site. How can this ratio be tuned in experiments? As mentioned in the previous section, Feshbach resonances[65] allow one to tune the scattering length of the atoms directly and thereby tune the on-site matrix element U (ref. 66). Another route to strong interactions is to quench the kinetic energy of the atoms $J \to 0$ by increasing the optical-lattice depth[64]. Both methods have been used in experiments to drive the system into a Mott insulating regime.

For an equal mixture of spin-1/2 fermions, density fluctuations become suppressed in a similar way, owing to the strong interactions between the particles, and a fermionic Mott insulator is formed[67,68]. In this strong interaction regime ($U/J \gg 1$), superexchange processes provide the basic mechanism for an antiferromagnetic coupling between spins on neighbouring lattice sites[69,70]. However, so far the overall entropies achieved in

Box 2 | High-resolution imaging.

High-resolution fluorescence imaging has opened a new avenue for the investigation of ultracold quantum gases. How is an atomic-resolution image taken in the experiment? Imagine having prepared a many-body quantum phase in an optical lattice. To observe the atoms in this phase, near-resonant light is turned on, such that the atoms start fluorescing. As shown in Fig. B2a, the laser-induced fluorescence is captured by a high-resolution microscope objective and imaged onto a low-noise CCD (charge-coupled device) camera. To achieve a good signal-to-noise ratio — such that a single atom can be clearly discerned from the background — a few thousand scattered photons per atom must be detected on the camera. To achieve such high scattering rates and simultaneously preserve the position of the atom during imaging, the depth of the optical lattice is increased during the imaging process by a factor of $\times 100$, so that the atoms remain confined to their original lattice sites. Laser cooling during the imaging process helps keep the temperature of the atoms well below the lattice depth. One can thereby avoid thermal hopping of the atoms, a process which would hinder the faithful reconstruction of the initial spatial atom distribution.

Detecting individual atoms with an optical resolution higher than the lattice spacing amounts to a projective measurement of the local occupation $\hat{n}_i$ of different lattice sites. Such a projective measurement begins as soon as the first photons are scattered from the atoms. In the experiments, a further complication arises: if two atoms are confined to within an optical wavelength λ of an optical transition and near-resonant light of this wavelength is shone onto the atoms, both atoms are rapidly expelled from the trap, owing to light-induced collisions[144]. As shown in Fig. B2b, because atoms are only lost pairwise in such a process, the imaged occupation reflects the parity of the lattice occupation $\hat{s}_i = \hat{n}_i \bmod 2$.

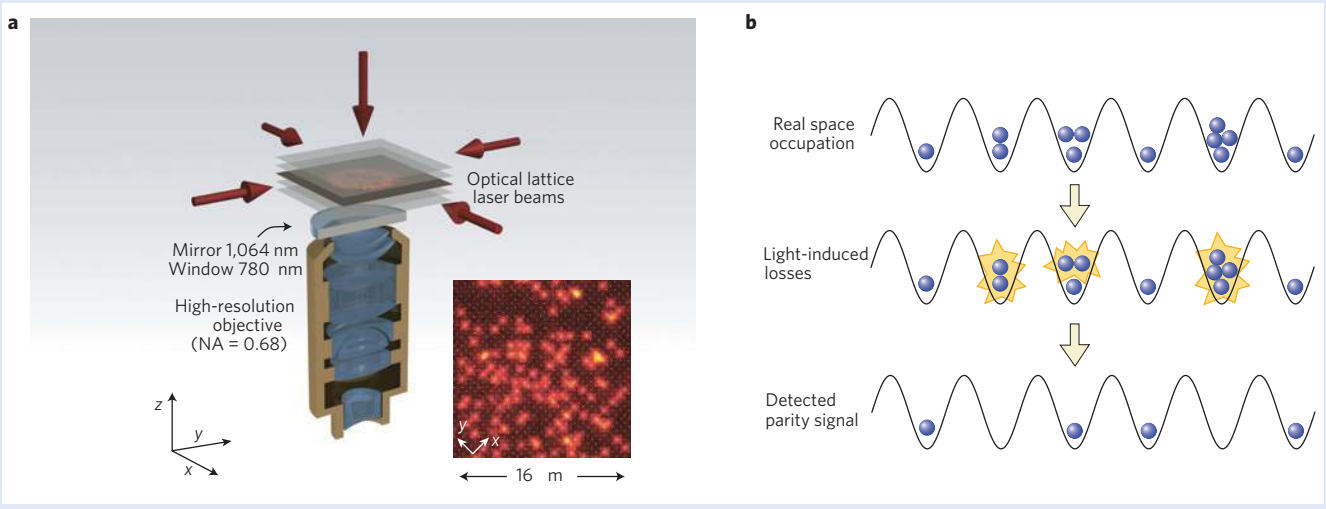

Figure B2 | High-resolution imaging of ultracold atoms in an optical lattice. a, A high-resolution microscope images the laser-induced fluorescence of atoms trapped in a single plane of an optical lattice. Panel reproduced from ref. 80. **b**, As a result of light-induced losses, atoms trapped in the same well are lost in pairs, resulting in a parity detection of the atomic on-site occupancy.

experiments have not been low enough to observe such a many-body quantum antiferromagnet that could form the basis for studies related to high-T_c superconductivity within the Hubbard model[58]. The higher spin entropy capacity of alkaline earth atoms, with their N multiple internal spin states and $SU(N)$ symmetric interactions, could facilitate the production of magnetically ordered phases[71]. At the same time, such experiments could provide insight into the nature of the magnetic ordering in these unconventional high-spin states[72], which remains a challenging problem for theory[73]. In the large-N limit, these systems are expected to form a chiral spin liquid with topological order and Abelian fractional statistics[74]. Irrespective of the atomic species, one of the major challenges in the field is to devise novel cooling (or better entropy-removal) schemes. In addition, a thorough understanding of technically induced heating rates is needed[75]. Fortunately, a dramatic development on the detection and manipulation side of ultracold quantum gases might just hold the answer to how both goals can be achieved.

During the past two years, a new way to image ultracold quantum gases *in situ* and with highest optical resolution has been established which holds the promise to revolutionize the field of quantum simulations with ultracold atoms. In previous experiments, one mainly used time-of-flight images after releasing the quantum gases from the trapping potential. This provided insight into the momentum distribution and coherence properties of the many-body phases in the lattice[46]. Now, high-resolution absorption[76,77], fluorescence[78–80] and electron microscope-based images[81] of the trapped density distribution of a quantum gas have become available to experimentalists. As an example, we discuss in more detail the case of high-resolution fluorescence imaging (Box 2). Such images have provided access to single-atom resolved distributions of particles on a lattice[79,80]. Taking a snapshot of the quantum gas amounts to a projective measurement of the many-body quantum system onto the parity of the local occupation number $\hat{s}_i = \hat{n}_i \bmod 2$ (Box 2). Examples of such a measurement of a BEC and atomic-limit Mott insulators are shown in Fig. 2. One of the amazing aspects of this imaging technique is that it not only allows us to capture the average particle-number distribution, but also to reveal complex spatial correlations between the particles by analysing as a set of single snapshots of the quantum gas. One can thereby gain access to thermal and quantum fluctuations of the system at the level of single excitations, enabling, for example, thermometry in the lattice down to the 50 pK level[80]. Furthermore, complex non-local quantum correlations and hidden order parameters can be measured in this way. A recent example is

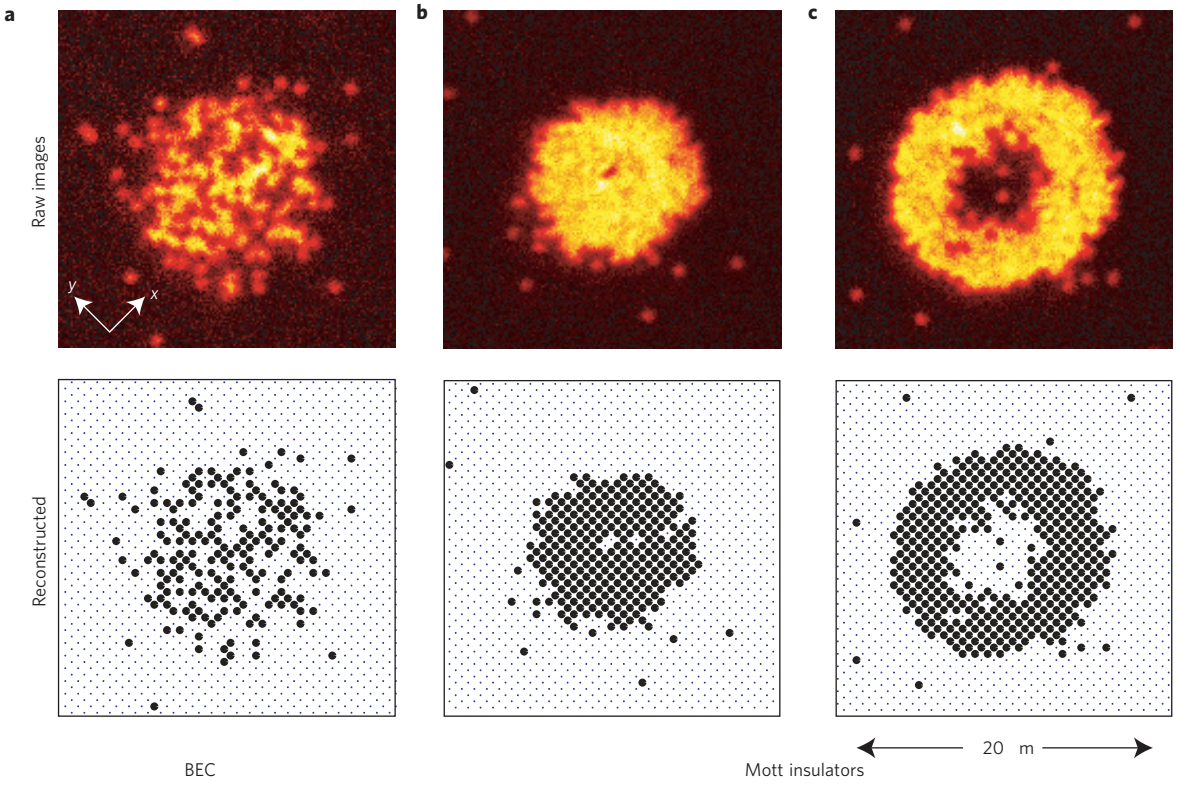

Figure 2 | Single-atom resolved images of a BEC and Mott insulators. a, A weakly interacting BEC. **b**,**c**, Strongly interacting Mott insulators in the atomic limit. The top row shows the raw-data fluorescence images. For higher atom numbers (**c**) a shell structure develops with a doubly occupied core in the centre. Owing to light-induced losses, the parity of the occupation number is detected in experiments (Box 2). The bottom row shows the results of an image-analysis algorithm through which the particle positions were reconstructed. Figure reproduced from ref. 80.

the observation of string order in one-dimensional Bose gases[82,83]. By introducing longer-ranged interactions using Rydberg atoms[84,85] or polar molecules[86] one could thus hope to realize and detect novel topological quantum phases, such as a Haldane insulator in one dimension[82,87], which exhibits a hidden antiferromagnetic ordering.

The high-resolution optics employed to image the quantum gases can also be used for single-site-resolved spin control. Here, a laser beam is focussed through the objective onto the atoms and microwaves are used to coherently flip the spin of a single atom at a predetermined lattice site[88]. Almost any possible spin structure can thereby be prepared in the lattice (Fig. 3). In the near future it is conceivable that arbitrary potential landscapes and spin patterns will be created by projecting highly structured light fields onto the atoms using spatial light modulators. These might, in fact, be the enabling step required for a novel cooling approach, where high-entropy regions are addressed and removed or separated by potential barriers from a low-entropy core[89,90]. A first step in this respect was recently achieved by making use of an orbital interaction-blockade effect to remove entropy from the gas[91,92].

Another possibility to realize quantum magnetism with cold atoms is to abandon superexchange interactions completely, thus avoiding their lower energy scales, and work in a pseudo-spin model, where spin components are implemented as different occupations of lattice sites. In this way, for example, it was possible to expose a unit-filling Mott insulator to a strong field. At field strengths where the energy difference between lattice sites matches the on-site interaction energy, atoms can start to resonantly tunnel to neighbouring wells. However, the tunnelling of one atom to the next well sets a constraint on how the next neighbour atom can tunnel, which can be effectively described by an antiferromagnetic Ising type interaction[93]. Using this mapping, the quantum Ising model was recently simulated and the resulting antiferromagnetic order in a one-dimensional chain directly observed[94,95] (Fig. 4). Extensions of this approach to higher dimensions could lead to the generation of exotic quantum-liquid states with no broken symmetry[96].

Artificial gauge fields

We now turn to our last example, starting with the following question: can one use atomic gases to simulate charged quantum many-body systems, such as an electron fluid in an external magnetic field? This looks, at first, to be demanding too much: as orbital magnetism is absent for neutral particles, the simulation of phenomena such as the quantum Hall effect seems to be out of reach. However, this apparent impossibility can be circumvented. For these gases, theoretical tools have been designed to emulate any coupling between matter and gauge potentials, and one emerging goal is now to address problems in quantum field theory.

Connecting cold atomic gases to quantum Hall physics has been the driving force in this emergent subject[97]. At the basis of the quantum Hall effect, one finds the very specific structure of the energy levels of a single electron confined in a plane in the presence of a large transverse magnetic field[98]. These levels form flat bands (Landau levels) with a macroscopic degeneracy and a non-trivial topology, with both these ingredients playing a crucial role. The flatness of the single-particle energy bands enhances the role of interactions, which are thus determinant for the structure of the many-body ground state in the case of fractional quantum Hall effect[99]. The band topology is characterized by a non-zero Chern index, which entails the quantization of the Hall conductance and the existence of edge states[100].

NATURE PHYSICS DOI:10.1038/NPHYS2259

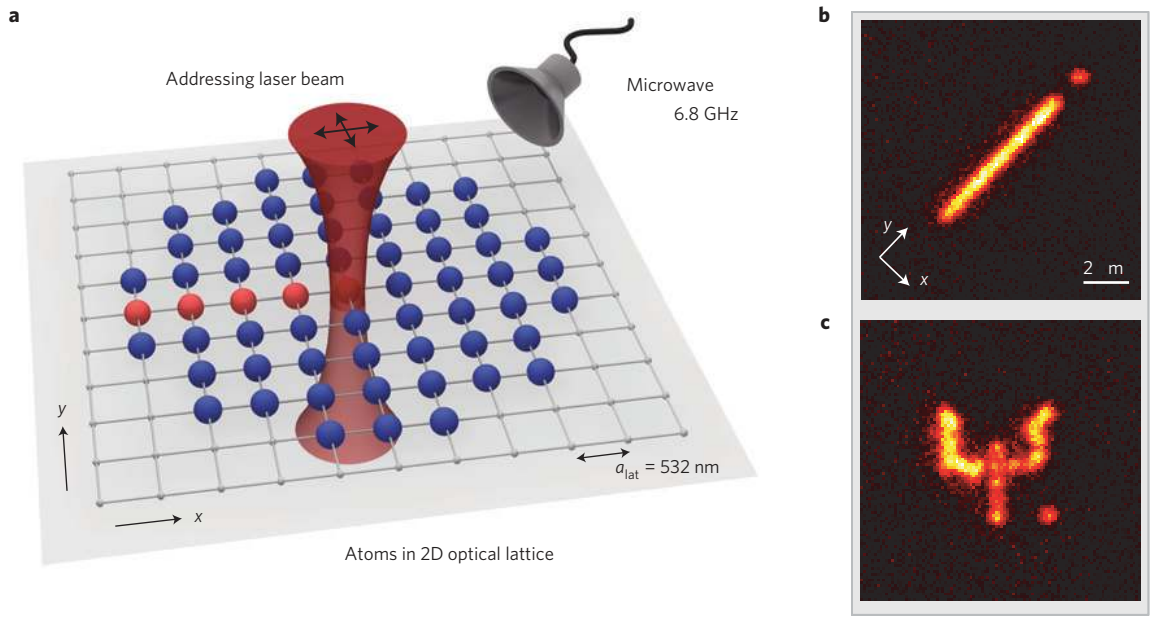

Figure 3 | Coherent control of single spins in an optical lattice. a, By focussing an addressing laser onto single atoms, the energy splitting between two spin states can be controlled. A microwave source, resonant only with this shifted transition frequency, allows single-site-resolved spin control. **b**,**c**, By moving the addressing beam to different lattice sites, arbitrary spin patterns at the single-spin level can be prepared. Figure reproduced from ref. 88.

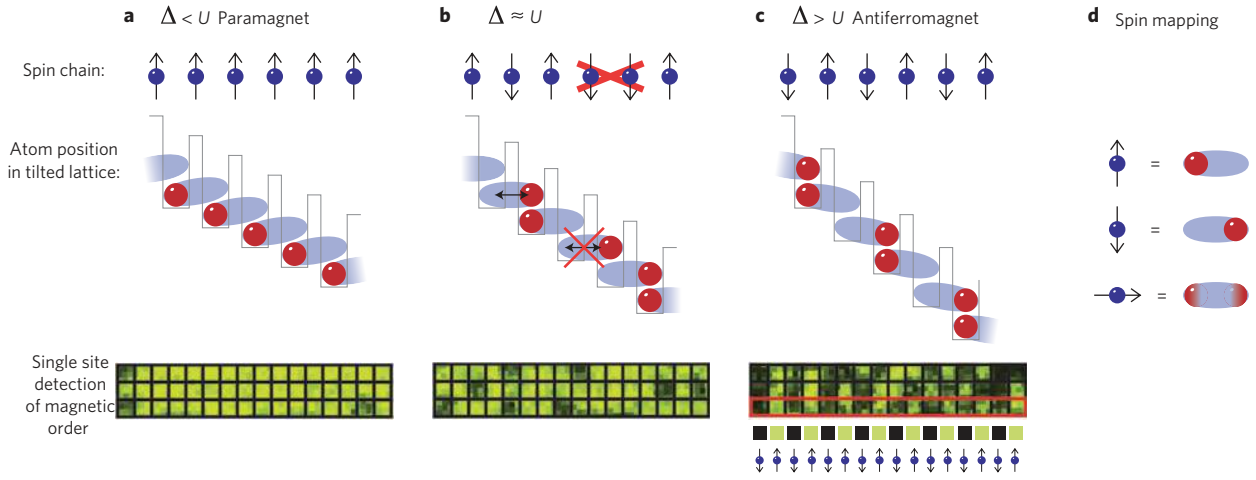

Figure 4 | Realization of a quantum Ising model using a one-dimensional Mott insulator in a strong potential gradient. When exposing a unit-filling Mott insulator to a potential gradient, neighbouring lattice sites are shifted in energy by Δ. For $\Delta < U$, the Mott insulator corresponds to a paramagnetic phase (**a**), whereas for $\Delta > U$ an antiferromagnetic phase is formed as the ground state of the system (**c**). A transition between both states occurs around $\Delta \approx U$ (**b**). The occupation of neighbouring sites represent pseudo-spins of the system (**d**). Lower row: direct single-site and single-atom resolved images of the transition from a paramagnetic to an antiferromagnetic phase. Panel reproduced from ref. 94.

Conceptually, the simplest way to obtain a Landau-like single-particle spectrum is to consider a bulk (continuous) gas confined in an isotropic 2D harmonic well, and rotate it at a frequency close to the trapping frequency. For superfluid atomic gases in the mean-field regime, this technique has already been used to study vortex physics[101,102]. In the context of quantum simulation, one must achieve a quasi-exact balance between trapping and centrifugal forces. This provides the required massive degeneracy of the single-particle ground state, with the remaining Coriolis force taking the role of the Lorentz force on a charge. The Hamiltonian of the atom gas is then formally identical to that of the electron fluid of the quantum Hall effect and one expects the ground state of the many-body system to be strongly correlated[97]. Experimentally, this route is well-adapted to small samples, say up to ten atoms, for which the balance between trapping and centrifugal forces can be performed with the required accuracy. The comparison with exact diagonalization methods, which can be performed for up to 10–15 particles, will be essential to validate the concept of quantum simulation in this framework. It could be performed for any density-correlation function that will be accessible using a detection scheme with single atom resolution (Box 2).

Cooling a rotating gas to a very low temperature is only one of the possible paths that have been proposed to reach a quantum Hall-like ground state. For a rotating fluid, one can also use a selective-dissipation process, such as atom loss due to three-body recombination, to favour some strongly correlated states[103]. Still another option is to smoothly vary an external parameter of the rotating system and rely on the fact that the system remains in

Box 3 | Implementing an artificial gauge field on a square optical lattice.

How can we realize a non-zero flux through the cells of a two-dimensional square optical lattice[117,145]? We consider, for simplicity, 'two-level atoms' with ground and excited states g and e, and we assume that both states are infinitely long-lived, that is, we neglect spontaneous emission processes. This approximation is an excellent one when dealing with alkaline-earth species or ytterbium atoms, which indeed possess in their spectrum excited states whose radiative lifetime exceeds the typical duration of a cold-gas experiment ($\sim$1 s). For the alkali-metal species that are more commonly used in experiments, the scheme can be transposed to two sublevels of the electronic ground-state, using optical Raman transitions[117].

The starting point of the implementation of the gauge field is the design of a state-dependent lattice potential (Fig. B3). Using laser standing waves with well-chosen frequencies, one can design the optical dipole potential such that the atom is trapped around the points $\mathbf{r}^{(g)}_{2n,m} = nd_x\mathbf{e}_x + md_y\mathbf{e}_y$ if it is in the internal state g, and $\mathbf{r}^{(e)}_{2n+1,m} = (n+1/2)d_x\mathbf{e}_x + md_y\mathbf{e}_y$ if it is in state e. This is achieved by tuning the laser creating the standing waves along the y and x axes to the so-called magic and anti-magic wavelengths, respectively. The magic wavelength (760 nm for Yb) is such that the optical dipole potential is the same for an atom in both states g and e, whereas these potentials are opposite for a laser tuned to the anti-magic wavelength (1,120 nm for Yb). The laser intensities are chosen such that the lattice operates in the tight-binding regime. More precisely, we suppose that the lattice periods d_x and d_y, which can be varied by changing the angles of the laser beams with respect to the z axis, are such that: the atom moves on the lattice along the y direction [$\mathbf{r}_{n,m} \rightarrow \mathbf{r}_{n,m\pm1}$] by standard tunnelling between adjacent sites; and the motion along x is frozen because of the large distance d_x between wells corresponding to the same internal state.

Suppose now that an additional laser beam, resonant with the g–e transition, propagates along the y axis. It is assumed to be a plane running wave $e^{i\phi}$ with phase $\phi = ky$. The atom initially in state g at position $\mathbf{r}^{(g)}_{2n,m}$ can jump to state e at position $\mathbf{r}^{(e)}_{2n\pm1,m}$ by absorbing a photon from this 'coupling laser' beam. On doing so, the phase of the laser at this location, $\phi = kmd_y$, is added to the phase of the atomic wavefunction (or subtracted in the reverse process where the atom jumps from e to g by stimulated emission of a photon). Consider, for example, the loop around the unit cell represented in Fig. B3:

$$g,\mathbf{r}^{(g)}_{2n,m} \xrightarrow{e^{ikmd_y}} e,\mathbf{r}^{(e)}_{2n+1,m} \xrightarrow{1} e,\mathbf{r}^{(e)}_{2n+1,m-1} \xrightarrow{e^{-ik(m-1)d_y}} g,\mathbf{r}^{(g)}_{2n,m-1} \xrightarrow{1} g,\mathbf{r}^{(g)}_{2n,m}$$

where we indicate above each arrow the phase gained by the atom. After travelling clockwise around this closed loop, we end up with a global phase change $\phi_{\text{cell}} = kd_y$. The situation is then similar to that of an electron moving on a square lattice, with a transverse magnetic field such that $B = \hbar\phi_{\text{cell}}/ed_xd_y$. In the present case the wavenumber of the coupling laser k is of the order of $2\pi/d_y$ and it can be fine-tuned by varying the angle of the coupling beam with respect to the z axis. The phase through the unit cell can therefore be adjusted to any value between 0 and 2π, allowing one to simulate arbitrarily large magnetic fields. Indeed, in this tight-binding model, two phases differing by an integer multiple of 2π lead to the same physical properties.

There is still one step left towards the simulation of orbital magnetism of electrons on a square lattice. The scheme which we outlined above actually leads to a staggered flux, with a phase alternating between $+kd_y$ and $-kd_y$ from one column to the next. Indeed, if we consider the cell next to that of Fig. B3 and also travel clockwise around this cell, we find:

$$g,\mathbf{r}^{(g)}_{2n,m} \xrightarrow{1} g,\mathbf{r}^{(g)}_{2n,m-1} \xrightarrow{e^{ik(m-1)dy}} e,\mathbf{r}^{(e)}_{2n-1,m-1} \xrightarrow{1} e,\mathbf{r}^{(e)}_{2n-1,m} \xrightarrow{e^{-ikmdy}} g,\mathbf{r}^{(g)}_{2n,m}$$

corresponding to the global phase change $-kd_y$. The staggered geometry is, of course, interesting in its own right[146,147] and corresponds to the implementation reported in ref. 124. However, the simulation of a uniform magnetic field with the same flux on each cell requires rectifying this effective field. The procedure for this is quite challenging in its practical implementation, but relatively simple in its principle[117,145]. One needs to send at least two coupling laser beams propagating in opposite directions along the y axis, with phases $\phi = \pm ky$. Using for instance the additional potential created by a superlattice of period 2 d_x, one lifts the degeneracy between the two transitions $g,\mathbf{r}^{(g)}_{2n,m} \rightarrow e,\mathbf{r}^{(e)}_{2n\pm1,m}$. One of these transitions is resonant with the laser beam with $\phi = ky$, and the other with the beam with $\phi = -ky$. In this way, the flux is the same on each cell ($\phi_{\text{cell}} = kd_y$), corresponding exactly to the model introduced in the seminal work of Hofstadter[122].

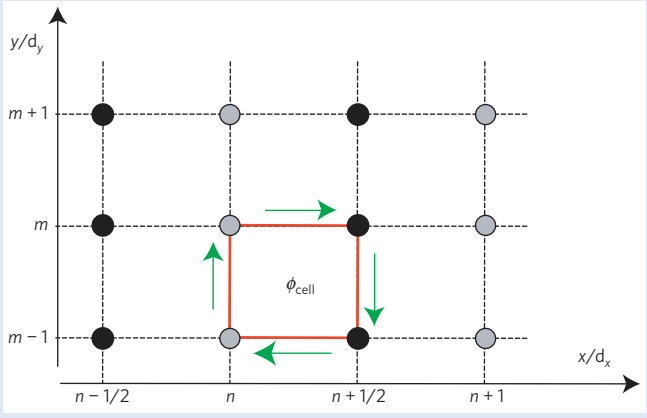

Figure B3 | Simulation of orbital magnetism with neutral atoms on a square optical lattice. The atoms are treated as two-level systems, with two internal states g and e. The lattice potential is state-dependent, with minima on the grey (or black) spots for an atom in state g (or e). Standard tunnelling allows the atom to move along the y axis. Motion along the x axis is possible by means of laser-assisted jumps, where the atom absorbs or emits a photon of a coupling laser propagating along y. In an absorption (or stimulated emission) process, the phase of the coupling laser is added to (or subtracted from) the phase of the atomic wave function. This leads to a non-zero phase ϕ_{cell} when the atom travels over the closed loop around the elementary cell of the lattice.

its ground state during the evolution; for example, deforming the trapping potential from a Mexican-hat shape into harmonic may provide a robust way to reach some emblematic states of fractional quantum Hall physics, such as the Laughlin wavefunction[104].

Atom–light interaction provides alternative routes to rotations for the simulation of orbital magnetism. One of them is directly inspired by the geometric Berry's phase[105], which appears when a quantum particle with several internal states evolves slowly enough to follow adiabatically one of these states[106–109]. Consider, for example, a two-level atom with ground (g) and excited (e) states that are coupled by a laser beam. If the phase and the intensity of the laser beam are spatially varying quantities, the eigenstates of the atom–light interaction (the so-called dressed states) are linear combinations of g and e that also vary in space. One can

tailor their space dependence and adjust the corresponding Berry's phase to mimic the Aharonov–Bohm phase acquired by a charged particle in a magnetic field. This method has recently led to the observation of vortices in a gas in the mean-field regime[110] and was subsequently extended to generate a spin–orbit coupling[111], a first step towards the simulation of a topological insulator and/or superconductor[112,113] with cold gases[114–116].

Atom–laser interactions are also well-suited for implementing an artificial gauge field in an optical lattice[117–120]. Consider, for example, a two-level atom moving on a two-dimensional square lattice which is state-dependent; that is, the energy minima are located on the columns with even (or odd) indices if the atom is in state g (or e). By using laser beams to drive the g–e transition, one can induce laser-assisted hopping between the odd and even sublattices[121]. By writing the appropriate phases on these laser beams (Box 3), one can reach a situation where a non-zero phase is accumulated by an atom when it travels on a closed contour encircling an elementary cell of the lattice[117]. This phase simulates a magnetic flux through the cell. It can take, in practice, any value between 0 and 2π, corresponding to arbitrarily large strengths of the effective magnetic field.

When the flux is the same through each plaquette of the lattice, the single particle spectrum is predicted to have a remarkable fractal structure, known as the Hofstadter butterfly[122]. Evidencing this structure with cold atoms would be an important achievement. Indeed, with real electrons on an Ångström-period lattice, the achievable fluxes per cell are too low to observe the main features of the butterfly, and its experimental observations so far have been obtained with larger systems, such as superconducting regular networks[123]. Very recently, a first step towards this goal was achieved in the cold-atom context, with the realization of a staggered flux which changes sign from one lattice cell to the next[124]. Another promising recent development is the notion of flux lattices[125,126]. There, one looks for a periodic configuration of laser light that leads to a single-particle spectrum as close as possible to the Landau spectrum, with a quasi-flat lowest band characterized by a non-zero Chern index. In contrast to the schemes aiming at observing the Hofstadter butterfly and operating in the tight-binding regime, flux lattices work in the weak-binding regime and require only low light intensity, thus reducing the spurious heating effect of photon scattering by the atomic gas.

Both bulk and lattices geometries can be used to implement richer gauge fields, including non-Abelian ones[127,128]: cold atom gases thus have the possibility to emulate not only electromagnetism, with quantum Hall-type phenomena, but also the more complex gauge fields which appear in high-energy physics. To simulate a non-Abelian gauge field, one can use a configuration where several dressed states form a degenerate manifold at every point in space. When the atom prepared in a state of this manifold slowly moves along a closed trajectory, its final state belongs to the manifold, but may differ from the initial state. The motional effect is thus not described by a simple Aharonov–Bohm phase, but by a matrix acting inside the manifold; two different closed paths may lead to non-commuting matrices, hence the non-Abelian structure of the gauge field[129,130].

In the perspective of quantum simulation, an important extension of these ideas is the realization of an artificial dynamical gauge field whose temporal evolution is coupled to the gas. To realize such a scheme one can think of replacing the beams causing laser-assisted hopping between adjacent sites of a lattice by the quantized modes of an optical cavity. The flux through a given cell of the lattice then becomes a quantum-dynamical variable related to the degrees of freedom of the cavity mode. This scheme can provide proof-of-principle experiments with one or a few plaquettes, but it is probably challenging to scale it to large systems, as the number of required cavities grows as the number of plaquettes. A second route is based on the coupling of the gas with other material particles[131]. One can consider a scheme where one species of particles (A) moves on the vertices of a lattice, while another species of particles (B), with its own degrees of freedom, is located on the lattice edges and controls the tunnelling matrix elements of the particles of species A. With such a device at hand, one would be able to perform analog quantum simulation of lattice gauge theories, a very challenging task indeed.

In this review article we have presented a few topics that illustrate the range of possibilities offered by cold atomic gases in terms of quantum simulation, from engineering the single-particle Hamiltonian to controlling interactions, in association with the ability to resolve and address single atoms in an optical lattice. Of course, these topics do not cover all the perspectives opened by systems based on atomic gases. Among other topics that are currently intensively studied, one should mention (1) the effect of controlled disorder, in connection with Anderson localization and spin glasses[132–135], (2) controlled long-range interactions with Rydberg atoms[84,85] or polar molecules[86] in an optical lattice, which could form the basis an *a priori* scalable quantum computer, and (3) controlled few-body collisions, which has recently led to novel insights into the quantum few-body problem[136]. In all cases the unprecedented precision in the control of cold atomic and molecular gases is the key to obtaining insights into some fundamental, still-pending questions on quantum matter. We conclude by mentioning just one of these questions: calculating exactly the time evolution of a strongly correlated system just after a quench, for example, is a notoriously difficult (and in many cases still intractable) task for numerical simulations[137]. Experiments with atomic gases may play a key role in addressing this problem and offer a unique chance of identifying as yet unknown universal regimes in many-body dynamics[138,139].

References

1. Feynman, R. P. Simulating physics with computers. *Int. J. Theor. Phys.* **21,** 467–488 (1982).
2. Inguscio, M., Ketterle, W. & Salomon, C. *Ultra-cold Fermi Gases: Proceedings of the International School of Physics* 'Enrico Fermi', course clxiv, Varenna (2008).
3. Randeria, M., Zwerger, W. & Zwierlein, M. (eds) in *The BCS–BEC Crossover and the Unitary Fermi Gas* Vol. 836 (Lecture Notes in Physics, Springer, 2012).
4. Giorgini, S., Pitaevskii, L. P. & Stringari, S. Theory of ultracold atomic Fermi gases. *Rev. Mod. Phys.* **80,** 1215–1274 (2008).
5. Bardeen, J., Cooper, L. & Schrieffer, J. Theory of superconductivity. *Phys. Rev.* **108,** 1175–1204 (1957).
6. Petrov, D., Salomon, C. & Shlyapnikov, G. Weakly bound dimers of fermionic atoms. *Phys. Rev. Lett.* **93,** 090404 (2004).
7. Werner, F. & Castin, Y. Unitary quantum three-body problem in a harmonic trap. *Phys. Rev. Lett.* **97,** 150401 (2006).
8. Tan, S. Large momentum part of a strongly correlated Fermi gas. *Ann. Phys.* **323,** 2971–2986 (2008).
9. Ho, T. Universal thermodynamics of degenerate quantum gases in the unitarity limit. *Phys. Rev. Lett.* **92,** 090402 (2004).
10. Bertsch, G. in *Proceedings of the Tenth International Conference on Recent Progress in Many-Body Theories* (eds Bishop, R., Gernoth, K. A., Walet, N. R. & Xian, Y.) (World Scientific, 2000).
11. O'Hara, K., Hemmer, S., Gehm, M., Granade, S. & Thomas, J. Observation of a strongly interacting degenerate Fermi gas of atoms. *Science* **298,** 2179–2182 (2002).
12. Bourdel, T. *et al.* Experimental study of the BEC–BCS crossover region in lithium 6. *Phys. Rev. Lett.* **93,** 050401 (2004).
13. Stewart, J., Gaebler, J., Regal, C. & Jin, D. Potential energy of a ^{40}K Fermi gas in the BCS–BEC crossover. *Phys. Rev. Lett.* **97,** 220406 (2006).
14. Bartenstein, M. *et al.* Crossover from a molecular Bose–Einstein condensate to a degenerate Fermi gas. *Phys. Rev. Lett.* **92,** 120401 (2004).
15. Partridge, G., Li, W., Kamar, R., Liao, Y. & Hulet, R. Pairing and phase separation in a polarized Fermi gas. *Science* **311,** 503–505 (2006).
16. Joseph, J. *et al.* Measurement of sound velocity in a Fermi gas near a Feshbach resonance. *Phys. Rev. Lett.* **98,** 170401 (2007).
17. Kinast, J. *et al.* Heat capacity of a strongly interacting Fermi gas. *Science* **307,** 1296–1299 (2005).

18. Navon, N., Nascimbène, S., Chevy, F. & Salomon, C. The equation of state of a low-temperature Fermi gas with tunable interactions. *Science* **328,** 729–732 (2010).
19. Ku, M. J. H., Sommer, A. T., Cheuk, L. W. & Zwierlein, M. W. Revealing the superfluid Lambda transition in the universal thermodynamics of a unitary Fermi gas. *Science* **335,** 563–567 (2012).
20. Carlson, J., Chang, S., Pandharipande, V. & Schmidt, K. Superfluid Fermi gases with large scattering length. *Phys. Rev. Lett.* **91,** 050401 (2003).
21. Astrakharchik, G., Boronat, J., Casulleras, J. & Giorgini, S. Equation of state of a Fermi gas in the BEC–BCS crossover: A quantum Monte Carlo study. *Phys. Rev. Lett.* **93,** 200404 (2004).
22. Altmeyer, A. *et al.* Precision measurements of collective oscillations in the BEC–BCS crossover. *Phys. Rev. Lett.* **98,** 040401 (2007).
23. Astrakharchik, G. E., Combescot, R., Leyronas, X. & Stringari, S. Equation of state and collective frequencies of a trapped Fermi gas along the BEC–unitarity crossover. *Phys. Rev. Lett.* **95,** 030404 (2005).
24. Nascimbène, S. *et al.* Fermi-liquid behavior of the normal phase of a strongly interacting gas of cold atoms. *Phys. Rev. Lett.* **106,** 215303 (2011).
25. Sommer, A., Ku, M., Roati, G. & Zwierlein, M. Universal spin transport in a strongly interacting Fermi gas. *Nature* **472,** 201–204 (2011).
26. Zwierlein, M., Schirotzek, A., Schunck, C. & Ketterle, W. Fermionic superfluidity with imbalanced spin populations. *Science* **311,** 492–496 (2006).
27. Shin, Y., Schunck, C., Schirotzek, A. & Ketterle, W. Phase diagram of a two-component Fermi gas with resonant interactions. *Nature* **451,** 689–693 (2008).
28. Shin, Y. Determination of the equation of state of a polarized Fermi gas at unitarity. *Phys. Rev. A* **77,** 041603 (2008).
29. Schirotzek, A., Wu, C., Sommer, A. & Zwierlein, M. Observation of Fermi polarons in a tunable Fermi liquid of ultracold atoms. *Phys. Rev. Lett.* **102,** 230402 (2009).
30. Nascimbene, S. *et al.* Collective oscillations of an imbalanced Fermi gas: Axial compression modes and polaron effective mass. *Phys. Rev. Lett.* **103,** 170402 (2009).
31. Haussmann, R. Properties of a Fermi liquid at the superfluid transition in the crossover region between BCS superconductivity and Bose–Einstein condensation. *Phys. Rev. B* **49,** 12975–12983 (1994).
32. Chen, Q., Stajic, J., Tan, S. & Levin, K. BCS–BEC crossover: From high temperature superconductors to ultracold superfluids. *Phys. Rep.* **412,** 1–88 (2005).
33. Burovski, E., Prokof'ev, N., Svistunov, B. & Troyer, M. Critical temperature and thermodynamics of attractive fermions at unitarity. *Phys. Rev. Lett.* **96,** 160402 (2006).
34. Bulgac, A., Drut, J. & Magierski, P. Spin 1/2 fermions in the unitary regime: A superfluid of a new type. *Phys. Rev. Lett.* **96,** 090404 (2006).
35. Hu, H., Liu, X. & Drummond, P. Equation of state of a superfluid Fermi gas in the BCS–BEC crossover. *Europhys. Lett.* **74,** 574–580 (2006).
36. Haussmann, R., Rantner, W., Cerrito, S. & Zwerger, W. Thermodynamics of the BCS–BEC crossover. *Phys. Rev. A* **75,** 023610 (2007).
37. Combescot, R., Alzetto, F. & Leyronas, X. Particle distribution tail and related energy formula. *Phys. Rev. A* **79,** 053640 (2009).
38. Luo, L., Clancy, B., Joseph, J., Kinast, J. & Thomas, J. Measurement of the entropy and critical temperature of a strongly interacting Fermi gas. *Phys. Rev. Lett.* **98,** 080402 (2007).
39. Horikoshi, M., Nakajima, S., Ueda, M. & Mukaiyama, T. Measurement of universal thermodynamic functions for a unitary Fermi gas. *Science* **327,** 442–445 (2010).
40. Nascimbène, S., Navon, N., Jiang, K., Chevy, F. & Salomon, C. Exploring the thermodynamics of a universal Fermi gas. *Nature* **463,** 1057–1060 (2010).
41. Van Houcke, K. *et al.* Feynman diagrams versus Feynman quantum emulator. Preprint at http://arxiv.org/abs/1110.3747 (2011).
42. Rupak, G. Universality in a 2-component Fermi system at finite temperature. *Phys. Rev. Lett.* **98,** 090403 (2007).
43. Liu, X., Hu, H. & Drummond, P. Virial expansion for a strongly correlated Fermi gas. *Phys. Rev. Lett.* **102,** 160401 (2009).
44. Rakshit, D., Daily, K. & Blume, D. Natural and unnatural parity states of small trapped equal-mass two-component Fermi gases at unitarity and fourth-order virial coefficient. Preprint at http://arxiv.org/abs/1106.5958 (2011).
45. Kohstall, C. *et al.* Metastability and coherence of repulsive polarons in a strongly interacting Fermi mixture. Preprint at http://arxiv.org/abs/1112.0020 (2011).
46. Bloch, I., Dalibard, J. & Zwerger, W. Many-body physics with ultracold gases. *Rev. Mod. Phys.* **80,** 885–964 (2008).
47. Petsas, K., Coates, A. & Grynberg, G. Crystallography of optical lattices. *Phys. Rev. A* **50,** 5173–5189 (1994).
48. Greiner, M., Bloch, I., Mandel, M. O., Hänsch, T. W. & Esslinger, T. Exploring phase coherence in a 2D lattice of Bose–Einstein condensates. *Phys. Rev. Lett.* **87,** 160405 (2001).
49. Sebby-Strabley, J., Anderlini, M., Jessen, P. & Porto, J. Lattice of double wells for manipulating pairs of cold atoms. *Phys. Rev. A* **73,** 033605 (2006).
50. Fölling, S. *et al.* Direct observation of second-order atom tunnelling. *Nature* **448,** 1029–1032 (2007).
51. Becker, C. *et al.* Ultracold quantum gases in triangular optical lattices. *New J. Phys.* **12,** 065025 (2010).
52. Tarruell, L., Greif, D., Uehlinger, T., Jotzu, G. & Esslinger, T. Creating, moving and merging Dirac points with a Fermi gas in a tunable honeycomb lattice. Preprint at http://arxiv.org/abs/1111.5020 (2011).
53. Jo, G-B. *et al.* Ultracold atoms in a tunable optical kagome lattice. *Phys. Rev. Lett.* **108,** 045305 (2011).
54. Grossmann, F., Dittrich, T., Jung, P. & Hänggi, P. Coherent destruction of tunneling. *Phys. Rev. Lett.* **67,** 516–519 (1991).
55. Eckardt, A., Weiss, C. & Holthaus, M. Superfluid-insulator transition in a periodically driven optical lattice. *Phys. Rev. Lett.* **95,** 260404 (2005).
56. Lignier, H. *et al.* Dynamical control of matter-wave tunneling in periodic potentials. *Phys. Rev. Lett.* **99,** 220403 (2007).
57. Struck, J. *et al.* Quantum simulation of frustrated classical magnetism in triangular optical lattices. *Science* **333,** 996–999 (2011).
58. Lee, P., Nagaosa, N. & Wen, X-G. Doping a Mott insulator: Physics of high-temperature superconductivity. *Rev. Mod. Phys.* **78,** 17–85 (2006).
59. Jaksch, D. & Zoller, P. The cold atoms Hubbard toolbox. *Ann. Phys.* **315,** 52–79 (2005).
60. Lewenstein, M. *et al.* Ultracold atomic gases in optical lattices: Mimicking condensed matter physics and beyond. *Adv. Phys.* **56,** 243–379 (2007).
61. Esslinger, T. Fermi–Hubbard physics with atoms in an optical lattice. *Annu. Rev. Condens. Mater. Phys.* **1,** 129–152 (2010).
62. Fisher, M. P. A., Weichman, P. B., Grinstein, G. & Fisher, D. S. Boson localization and the superfluid-insulator transition. *Phys. Rev. B* **40,** 546–570 (1989).
63. Jaksch, D., Bruder, C., Cirac, J., Gardiner, C. & Zoller, P. Cold bosonic atoms in optical lattices. *Phys. Rev. Lett.* **81,** 3108–3111 (1998).
64. Greiner, M., Mandel, O., Esslinger, T., Hänsch, T. W. & Bloch, I. Quantum phase transition from a superfluid to a Mott insulator in a gas of ultracold atoms. *Nature* **415,** 39–44 (2002).
65. Chin, C., Grimm, R., Julienne, P. & Tiesinga, E. Feshbach resonances in ultracold gases. *Rev. Mod. Phys.* **82,** 1225–1286 (2010).
66. Mark, M. *et al.* Precision measurements on a tunable Mott insulator of ultracold atoms. *Phys. Rev. Lett.* **107,** 175301 (2011).
67. Jördens, R., Strohmaier, N., Günter, K., Moritz, H. & Esslinger, T. A Mott Insulator of fermionic Atoms in an optical lattice. *Nature* **455,** 204–207 (2008).
68. Schneider, U. *et al.* Metallic and insulating phases of repulsively interacting fermions in a 3D optical lattice. *Science* **322,** 1520–1525 (2008).
69. Auerbach, A. *Interacting Electrons and Quantum Magnetism* (Springer, 1994).
70. Trotzky, S. *et al.* Time-resolved observation and control of superexchange interactions with ultracold atoms in optical lattices. *Science* **319,** 295–299 (2008).
71. Hazzard, K., Gurarie, V., Hermele, M. & Rey, A. High temperature thermodynamics of fermionic alkaline earth atoms in optical lattices. Preprint at http://arxiv.org/abs/1011.0032 (2010).
72. Gorshkov, A. V. *et al.* Two-orbital SU(N) magnetism with ultracold alkaline-earth atoms. *Nature Phys.* **6,** 289–295 (2010).
73. Corboz, P., Läuchli, A., Penc, K., Troyer, M. & Mila, F. Simultaneous dimerization and SU(4) symmetry breaking of 4-color fermions on the square lattice. *Phys. Rev. Lett.* **107,** 215301 (2011).
74. Hermele, M., Gurarie, V. & Rey, A. Mott insulators of ultracold fermionic alkaline earth atoms: Underconstrained magnetism and chiral spin liquid. *Phys. Rev. Lett.* **103,** 135301 (2009).
75. Pichler, H., Daley, A. & Zoller, P. Nonequilibrium dynamics of bosonic atoms in optical lattices: Decoherence of many-body states due to spontaneous emission. *Phys. Rev. A* **82,** 063605 (2010).
76. Gemelke, N., Zhang, X., Hung, C-L. & Chin, C. In situ observation of incompressible Mott-insulating domains in ultracold atomic gases. *Nature* **460,** 995–998 (2009).
77. Zimmermann, B., Müller, T., Meineke, J., Esslinger, T. & Moritz, H. High-resolution imaging of ultracold fermions in microscopically tailored optical potentials. *New J. Phys.* **13,** 043007 (2011).
78. Nelson, K., Li, X. & Weiss, D. Imaging single atoms in a three-dimensional array. *Nature Phys.* **3,** 556–560 (2007).
79. Bakr, W. S. *et al.* Probing the superfluid-to-Mott insulator transition at the single-atom level. *Science* **329,** 547–550 (2010).
80. Sherson, J. F. *et al.* Single-atom-resolved fluorescence imaging of an atomic Mott insulator. *Nature* **467,** 68–72 (2010).
81. Gericke, T., Würtz, P., Reitz, D., Langen, T. & Ott, H. High-resolution scanning electron microscopy of an ultracold quantum gas. *Nature Phys.* **4,** 949–953 (2008).

82. Berg, E., Dalla Torre, E., Giamarchi, T. & Altman, E. Rise and fall of hidden string order of lattice bosons. *Phys. Rev. B* **77,** 245119 (2008).
83. Endres, M. *et al.* Observation of correlated particle-hole pairs and string order in low-dimensional Mott insulators. *Science* **334,** 200–203 (2011).
84. Saffman, M., Walker, T. & Mølmer, K. Quantum information with Rydberg atoms. *Rev. Mod. Phys.* **82,** 2313–2363 (2010).
85. Löw, R. *et al.* An experimental and theoretical guide to strongly interacting Rydberg gases. Preprint at http://arxiv.org/abs/1202.2871 (2012).
86. Carr, L., DeMille, D., Krems, R. & Ye, J. Cold and ultracold molecules: science, technology and applications. *New J. Phys.* **11,** 055049 (2009).
87. Dalla Torre, E. G., Berg, E. & Altman, E. Hidden Order in 1D Bose Insulators. *Phys. Rev. Lett.* **97,** 260401 (2006).
88. Weitenberg, C. *et al.* Single-spin addressing in an atomic Mott insulator. *Nature* **471,** 319–324 (2011).
89. Ho, T-L. & Zhou, Q. Universal cooling scheme for quantum simulation. Preprint at http://arxiv.org/abs/0911.5506 (2009).
90. Bernier, J-S. *et al.* Cooling fermionic atoms in optical lattices by shaping the confinement. *Phys. Rev. A* **79,** 061601(R) (2009).
91. Rabl, P., Daley, A., Fedichev, P., Cirac, J. & Zoller, P. Defect-suppressed atomic crystals in an optical lattice. *Phys. Rev. Lett.* **91,** 110403 (2003).
92. Bakr, W. S. *et al.* Orbital excitation blockade and algorithmic cooling in quantum gases. *Nature* **480,** 500–503 (2011).
93. Sachdev, S., Sengupta, K. & Girvin, S. Mott insulators in strong electric fields. *Phys. Rev. B* **66,** 075128 (2002).
94. Simon, J. *et al.* Quantum simulation of antiferromagnetic spin chains in an optical lattice. *Nature* **472,** 307–312 (2011).
95. Ma, R. *et al.* Photon-assisted tunneling in a biased strongly correlated Bose gas. *Phys. Rev. Lett* **107,** 095301 (2011).
96. Pielawa, S., Kitagawa, T., Berg, E. & Sachdev, S. Correlated phases of bosons in tilted frustrated lattices. *Phys. Rev. B* **83,** 205135 (2011).
97. Cooper, N. R. Rapidly rotating atomic gases. *Adv. Phys.* **57,** 539–616 (2008).
98. Landau, L. D. & Lifshitz, E. M. *Quantum Mechanics: Non-Relativistic Theory* (Pergamon Press, 1977).
99. Laughlin, R. B. Anomalous quantum Hall effect: An incompressible quantum fluid with fractionally charged excitations. *Phys. Rev. Lett.* **50,** 1395–1398 (1983).
100. Thouless, D. J., Kohmoto, M., Nightingale, M. P. & den Nijs, M. Quantized Hall conductance in a two-dimensional periodic potential. *Phys. Rev. Lett.* **49,** 405–408 (1982).
101. Fetter, A. L. Rotating trapped Bose–Einstein condensates. *Rev. Mod. Phys.* **81,** 647–691 (2009).
102. Schweikhard, V., Coddington, I., Engels, P., Mogendorff, V. P. & Cornell, E. A. Rapidly rotating Bose-Einstein condensates in and near the lowest Landau level. *Phys. Rev. Lett.* **92,** 040404 (2004).
103. Roncaglia, M., Rizzi, M. & Cirac, J. I. Pfaffian state generation by strong three-body dissipation. *Phys. Rev. Lett.* **104,** 096803 (2010).
104. Roncaglia, M., Rizzi, M. & Dalibard, J. From rotating atomic rings to quantum Hall states. *Sci. Rep.* **1,** 1–6 (2011).
105. Berry, M. V. Quantal phase factors accompanying adiabatic changes. *Proc. R. Soc. A* **392,** 45–57 (1984).
106. Dum, R. & Olshanii, M. Gauge structures in atom-laser interaction: Bloch oscillations in a dark lattice. *Phys. Rev. Lett.* **76,** 1788–1791 (1996).
107. Juzeliunas, G. & Öhberg, P. Slow light in degenerate Fermi gases. *Phys. Rev. Lett.* **93,** 033602 (2004).
108. Juzeliunas, G., Ruseckas, J., Öhberg, P. & Fleischhauer, M. Light-induced effective magnetic fields for ultracold atoms in planar geometries. *Phys. Rev. A* **73,** 025602 (2006).
109. Dalibard, J., Gerbier, F., Juzeliūnas, G. & Öhberg, P. Colloquium : Artificial gauge potentials for neutral atoms. *Rev. Mod. Phys.* **83,** 1523–1543 (2011).
110. Lin, Y-J., Compton, R. L., Jiménez-García, K., Porto, J. V. & Spielman, I. B. Synthetic magnetic fields for ultracold neutral atoms. *Nature* **462,** 628–632 (2009).
111. Lin, Y., Jiménez-Garcia, K. & Spielman, I. B. Spin-orbit-coupled Bose–Einstein condensates. *Nature* **471,** 83–86 (2011).
112. Hasan, M. & Kane, C. Colloquium: Topological insulators. *Rev. Mod. Phys.* **82,** 3045–3067 (2010).
113. Qi, X-L. & Zhang, S-C. Topological insulators and superconductors. *Rev. Mod. Phys.* **83,** 1057–1110 (2011).
114. Zhang, C., Tewari, S., Lutchyn, R. M. & Das Sarma, S. $p_x + ip_y$ superfluid from *s*-wave interactions of fermionic cold atoms. *Phys. Rev. Lett.* **101,** 160401 (2008).
115. Goldman, N. *et al.* Realistic time-reversal invariant topological insulators with neutral atoms. *Phys. Rev. Lett.* **105,** 255302 (2010).
116. Béri, B. & Cooper, N. R. $\mathbb{Z}_2$ topological insulators in ultracold atomic gases. *Phys. Rev. Lett.* **107,** 145301 (2011).
117. Jaksch, D. & Zoller, P. Creation of effective magnetic fields in optical lattices: The Hofstadter butterfly for cold neutral atoms. *New J. Phys.* **5,** 56 (2003).
118. Mueller, E. J. Artificial electromagnetism for neutral atoms: Escher staircase and Laughlin liquids. *Phys. Rev. A* **70,** 041603 (2004).
119. Sørensen, A. S., Demler, E. & Lukin, M. D. Fractional quantum Hall states of atoms in optical lattices. *Phys. Rev. Lett.* **94,** 086803 (2005).
120. Lim, L-K., Smith, C. M. & Hemmerich, A. Staggered-vortex superfluid of ultracold Bosons in an optical lattice. *Phys. Rev. Lett.* **100,** 130402 (2008).
121. Ruostekoski, J., Dunne, G. V. & Javanainen, J. Particle number fractionalization of an atomic Fermi–Dirac gas in an optical lattice. *Phys. Rev. Lett.* **88,** 180401 (2002).
122. Hofstadter, D. Energy levels and wave functions of Bloch electrons in rational and irrational magnetic fields. *Phys. Rev. B* **14,** 2239–2249 (1976).
123. Pannetier, B., Chaussy, J., Rammal, R. & Villegier, J. C. Experimental fine tuning of frustration: Two-dimensional superconducting network in a magnetic field. *Phys. Rev. Lett.* **53,** 1845–1848 (1984).
124. Aidelsburger, M. *et al.* Experimental realization of strong effective magnetic fields in an optical lattice. *Phys. Rev. Lett.* **107,** 255301 (2011).
125. Cooper, N. R. Optical flux lattices for ultracold atomic gases. *Phys. Rev. Lett.* **106,** 175301 (2011).
126. Cooper, N. R. & Dalibard, J. Optical flux lattices for two-photon dressed states. *Europhys. Lett.* **95,** 66004 (2011).
127. Ruseckas, J., Juzeliūnas, G., Öhberg, P. & Fleischhauer, M. Non-abelian gauge potentials for ultracold atoms with degenerate dark states. *Phys. Rev. Lett.* **95,** 010404 (2005).
128. Osterloh, K., Baig, M., Santos, L., Zoller, P. & Lewenstein, M. Cold atoms in non-abelian gauge potentials: From the Hofstadter 'Moth' to lattice gauge theory. *Phys. Rev. Lett.* **95,** 010403 (2005).
129. Wilczek, F. & Zee, A. Appearance of gauge structure in simple dynamical systems. *Phys. Rev. Lett.* **52,** 2111–2114 (1984).
130. Goldman, N. *Quantum Transport in Lattices Subjected to External Gauge Fields* (VDM Verlag, 2009).
131. Büchler, H., Hermele, M., Huber, S., Fisher, M. & Zoller, P. Atomic quantum simulator for lattice gauge theories and ring exchange models. *Phys. Rev. Lett.* **95,** 040402 (2005).
132. Sanchez-Palencia, L. & Lewenstein, M. Disordered quantum gases under control. *Nature Phys.* **6,** 87–95 (2010).
133. Billy, J. *et al.* Direct observation of Anderson localization of matter waves in a controlled disorder. *Nature* **453,** 891–894 (2008).
134. Roati, G. *et al.* Anderson localization of a non-interacting Bose-Einstein condensate. *Nature* **453,** 895–898 (2008).
135. Kondov, S. S., McGehee, W. R., Zirbel, J. J. & DeMarco, B. Three-dimensional Anderson localization of ultracold matter. *Science* **334,** 66–68 (2011).
136. Castin, Y. & Pricoupenko, L. (eds) The few body problem. *C. R. Phys.* **12,** 1–109 (2011).
137. Trotzky, S. *et al.* Probing the relaxation towards equilibrium in an isolated strongly correlated 1D Bose gas. *Nature Phys.* **8,** 325–330 (2012).
138. Polkovnikov, A., Sengupta, K., Silva, A. & Vengalattore, M. Colloquium: Nonequilibrium dynamics of closed interacting quantum systems. *Rev. Mod. Phys.* **83,** 863–883 (2011).
139. Lamacraft, A. & Moore, J. Potential insights into non-equilibrium behavior from atomic physics. Preprint at http://arXiv.org/abs/1106.3567 1–24 (2011).
140. Pilati, S. & Giorgini, S. Phase separation in a polarized Fermi gas at zero temperature. *Phys. Rev. Lett.* **100,** 030401 (2008).
141. Fuchs, J., Leyronas, X. & Combescot, R. Hydrodynamic modes of a one-dimensional trapped Bose gas. *Phys. Rev. A* **68,** 043610 (2003).
142. Ho, T. & Zhou, Q. Obtaining the phase diagram and thermodynamic quantities of bulk systems from the densities of trapped gases. *Nature Phys.* **6,** 131–134 (2009).
143. Spiegelhalder, F. *et al.* Collisional stability of ^{40}K immersed in a strongly interacting Fermi gas of ^{6}Li. *Phys. Rev. Lett.* **103,** 223203 (2009).
144. DePue, M. T. M., McCormick, C., Winoto, S. L., Oliver, S. & Weiss, D. D. S. Unity Occupation of Sites in a 3D Optical Lattice. *Phys. Rev. Lett.* **82,** 2262–2265 (1999).
145. Gerbier, F. & Dalibard, J. Gauge fields for ultracold atoms in optical superlattices. *New J. Phys.* **12,** 033007 (2010).
146. Möller, G. & Cooper, N. Condensed ground states of frustrated Bose–Hubbard models. *Phys. Rev. A* **82,** 063625 (2010).
147. Lim, L-K., Hemmerich, A. & Smith, C. M. Artificial staggered magnetic field for ultracold atoms in optical lattices. *Phys. Rev. A* **81,** 023404 (2010).

Acknowledgements

We thank P. Zoller and E. Altman for many useful discussions during the writing of this review article.

Additional information

The authors declare no competing financial interests. Reprints and permissions information is available online at www.nature.com/reprints. Correspondence and requests for materials should be addressed to I.B.